Int. J. Electrochem. Sci., 12 **(2017)** 1600 – 1611, doi: 10.20964/2017.02.58

International Journal of ELECTROCHEMICAL SCIENCE
www.electrochemsci.org

Electrochemical Corrosion Behavior of Fe64/Ni36 and Fe55/Ni45 Alloys in 4.0% Sodium Chloride Solutions

El-Sayed M. Sherif[1,2,*], *Hany S. Abdo*[1,3], *S. Zein El Abedin*[2]

[1]Deanship of Scientific Research, Advanced Manufacturing Institute, King Saud University, P. O. Box 800, Al-Riyadh 11421, Saudi Arabia
[2] Electrochemistry and Corrosion Laboratory, Physical Chemistry Department, National Research Centre, El Bohouth St. 33, Dokki, P.O. 12622, Giza, Egypt
[3] Mechanical Design and Materials Department, Faculty of Energy Engineering, Aswan University, Aswan 81521, Egypt
[*]E-mail: esherif@ksu.edu.sa

Received: 30 October 2016 / *Accepted:* 6 December 2016 / *Published:* 30 December 2016

The electrochemical corrosion behavior of two iron/nickel alloys namely, Fe64/Ni36 and Fe55/Ni45, in 4.0% NaCl solution was reported. The study was conducted using open-circuit potential, electrochemical impedance spectroscopy, cyclic polarization, and chronoamperometric current-time measurements. The surface of the alloys after 7 days immersion in the solution was investigated by scanning electron microscope and energy dispersive X-ray analyzer. It was found that the corrosion resistance for Fe55/Ni45 alloy was higher than that for Fe64/Ni36 one. This was confirmed by the low corrosion current and corrosion rate as well as the high corrosion resistance for Fe55/Ni45 compared to Fe64/Ni36 alloy. Moreover, the less negative potential and the low absolute current obtained for Fe55/Ni45 alloy by the open-circuit potential and chronoamperometric experiments, respectively.

Keywords: corrosion; iron-nickel alloys; polarization; EIS; chronoamperometry

1. INTRODUCTION

Nickel iron alloys have many characteristics that make it highly used in the industry. These include its good mechanical properties, low thermal expansion coefficient at lower temperatures, and its unique magnetic properties [1-4]. It is well known that iron-nickel alloys represent some of the most widely used super-alloys which used in a broad variety of applications, the majority of which involve corrosion and heat resistance; especially those have the nickel content in the range of 36% to 46%. It is

also known that Fe64/Ni36 alloy (Invar) has the lowest expansion of the Fe-Ni alloys; in atmospheric temperature and during normal variations, the alloy maintains almost constant dimensions [4-7].

The corrosion resistance of iron-nickel alloys undoubtedly depends on the content and amounts of Ni in the alloy [8-11]. It is reported that the iron nickel alloys have good corrosion resistance in oxidizing solutions. Seo et al. [12] studied the potentiodynamic polarization measurements for pure Fe and Fe-Ni alloys in acidic perchlorate solution to report the effect of Pb-underpotential deposition on its passivation and anodic dissolution [12]. It was found the addition of 10^{-3}Â M Pb^{2+} allows the potentials of these materials to move towards the positive direction leading to their passivation and inhibiting their anodic dissolutions. D. O. Condit [13] has investigated the corrosion of ten Fi-Ni alloys in sulfuric acid solution using potentiodynamic polarization technique and found that the anodic behavior in the active region of dissolution is controlled by the iron present in the alloys that contain up to 50at. % Ni. The author [12] reported the iron dissolves in the form ferrous state, +2, which is oxidized to the ferric state, +3. On the other hand, nickel dissolves in the +3 state at all anodic potentials [13]. Sayano and Nobe [14] also reported the electrochemical corrosion behavior of pure iron and nickel, 20%, 40%, 60%, and 80% Fe-Ni alloys in de-aerated 1N H_2SO_4 using anodic and cathodic polarization, weight loss and chemical analysis methods. This study [14] reported that the corrosion rate obtained by weight-loss and chemical analysis methods recorded the minimum value when the iron percentage was 40% due to the formation of an ordered structure of $FeNi_3$.

The objective of the present study was to evaluate the corrosion resistance results of two iron-nickel alloys (Fe64/Ni36 and Fe55/Ni45) and its measurements in 4.0% NaCl solution. The corrosion behavior after immersion in that solution for 40 min was performed using open-circuit potential, EIS, cyclic polarization, and change of chronoamperometric current with time at 50 mV (Ag/AgCl). The corroded surface of these materials after being immersed in the sodium chloride solutions for 7 days was analyzed using scanning electron microscope and energy dispersive X-ray analyzer.

2. EXPERIMENTAL

2.1. Test Solution and Electrochemical Cell

Sodium chloride (NaCl) was obtained from Merck with 99% purity and was used as received to prepare the 4.0% NaCl solution. A traditional electrochemical cell with three electrode configuration that accommodates for 300 cm^3 was used to perform all electrochemical experiments. The iron/nickel (Fe64/Ni36 and Fe55/Ni45) alloys, an Ag/AgCl electrode (in saturated KCl solution), and a platinum sheet were used as working, reference, and counter electrodes, respectively. The iron/nickel alloys were 6.0 mm diameter and were purchased from GoodFellow (Ermine Business Park, Huntingdon, England PE29 6WR). The working electrodes were prepared by welding to copper wires and mounted in epoxy resin and left for 24 h to dry in air. This process was carried out in order to allow only one surface of the electrodes to be exposed to the sodium chloride test solution. The surface of the iron/nickel alloys was polished and ground with different grades of emery papers before washing with

distilled water, cleaned with acetone and washed with distilled water again and finally immersed in the test solution to perform the electrochemical measurements as has been previously reported [14-17].

2.2. Electrochemical and surface investigation techniques

An Autolab workstation (Metrohm, Utrecht, Netherlands) was employed in obtaining the electrochemical data. The open-circuit potential (OCP) was measured versus time for 40 min. The electrochemical impedance spectroscopy (EIS) data were obtained after 40 min immersion in 4% NaCl solution from the open-circuit potential (E_{OCP}) value; the impedance parameters and the software have been reported earlier [15-18]. The potentiodynamic polarization curves were measured by scanning the potential from −1200 mV in the positive direction to 600 mV at a scan rate of 1 mV/s in regard to the Ag/AgCl reference electrode after 40 min immersion in the chloride test solution. The current-time curves were obtained after applying a value of 50 mV for 60 min on the iron/nickel electrodes after its immersion in the electrolytic solutions for 40 min. All experiments were carried out on a fresh surface of the iron/nickel electrodes. For surface investigations, the scanning electron microscope (SEM) micrographs and the profiles of the energy dispersive X-ray analyzer were obtained from the surface of the iron/nickel alloys after its immersion for 96 h in 4.0% NaCl solutions. Details of SEM/EDX instrumentations were the same as reported in our previous studies [16-18].

3. RESULTS AND DISCUSSION

3.1. Open-circuit potential

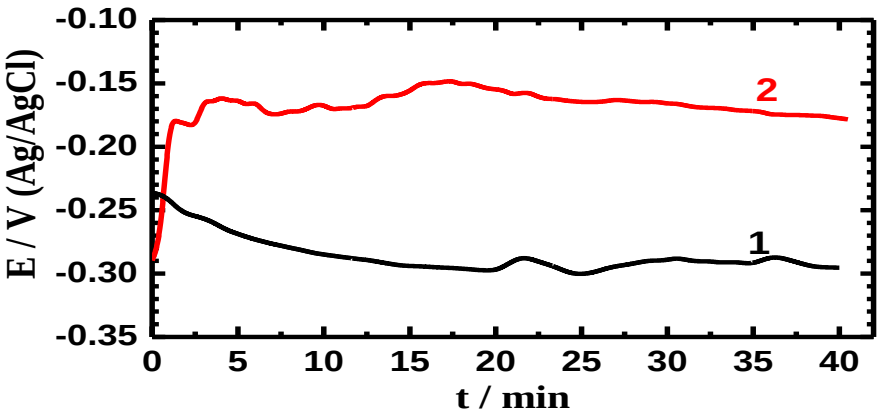

Figure 1. Potential-time curves obtained for (1) Fe64/Ni36 alloy and (2) Fe55/Ni45 alloy in 4% NaCl solutions.

Figure 1 presents the potential-time curves obtained for the iron/nickel alloys, (1) Fe64/Ni36 and (2) Fe55/Ni45, immersed in 4% NaCl solutions. It is seen that the potential of Fe64/Ni36 alloy slightly shifted towards the more negative values with time till the end of the run. This has resulted

from the dissolution of the surface of the alloy under the corrosiveness action of the ions present in the solution. On the other hand, the potential of Fe55/45Ni alloy abruptly shifted to the less negative potential upon its immersion in the test solution, which indicates on the thickening for a preformed oxide film. Prolonging the immersion time and up to 25 min led to a less negative shift in the potential, which is a result of either oxide film thickening or a formation of a passive film on the surface of the alloy. Increasing the immersion time longer than 25 min slightly increased the potential in the negative direction due to the dissolution of the formed film from the alloy's surface under the corrosiveness effect of the chloride ions [19]. The OCP experiments thus qualitatively show that the alloy that has high nickel content, Fe55/Ni45, has higher corrosion resistance than the low nickel content alloy, Fe64/Ni36.

3.2. Electrochemical impedance spectroscopy (EIS)

In order to report the kinetic parameters for the electron transfer at the iron/nickel alloy/NaCl solution interface, EIS measurements were carried out. The EIS technique has been employed in reporting the corrosion and protection against corrosion of metallic materials in harsh media [19-26]. Figure 2 shows the typical Nyquist plots obtained for iron/nickel alloys, (a) Fe64/Ni36 and (b) Fe55/Ni45 immersed in 4% NaCl solutions for 40 min. The spectra of Figure 2 say that only one semicircle is recorded for the iron/nickel alloys, the diameter of the semicircle obtained for Fe64/Ni36 is much smaller than that obtained for Fe55/Ni45 alloy. This qualitatively indicates that the alloy with high nickel content, Fe55/Ni45, has higher corrosion resistance than that for the low nickel content one, Fe64/Ni36.

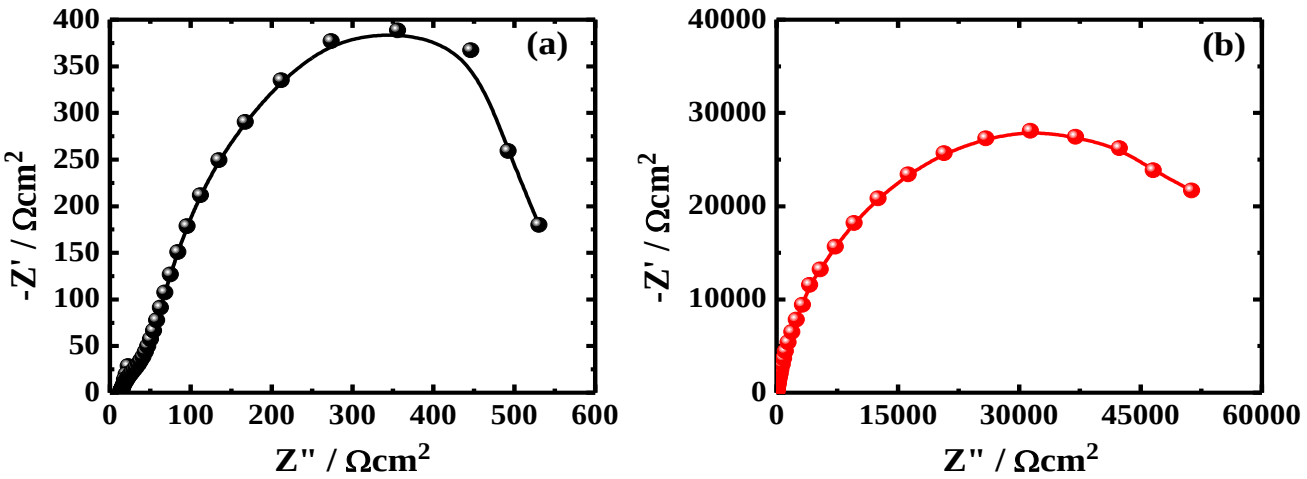

Figure 2. Typical Nyquist plots obtained for iron nickel alloys immersed in 4% NaCl solutions for 40 min (a) Fe64/Ni36 and (b) Fe55/Ni45.

We fitted the obtained EIS data to an equivalent circuit model that is shown in Figure 3. The symbols of the parameters shown on the equivalent circuit can be defined as well known as following; the solution resistance R_S, the constant phase elements Q, (Y_{Q1}, CPEs), the polarization resistance

between the surface of the alloys and NaCl solution interface R_{p1}, the double layer capacitance C_{dl}, and the polarization resistance that can also be defined as the charge transfer resistance R_{p2}.

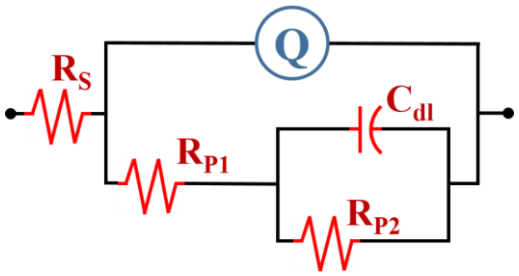

Figure 3. The equivalent circuit model used to fit EIS data shown in Figure 2.

Table 1 lists the values of the symbols of the equivalent circuit, which is depicted in Figure 3. It is seen from Table 1 that the values of surface and polarization resistances (R_S, R_{p1} and R_{p2}) Fe55/Ni45 alloy are higher than those obtained for Fe64/Ni36 alloy and reveals that the alloy with high nickel content has better resistance against corrosion in the chloride test solution. Moreover, Q, CPEs with their n component close to unity can be considered as double layer capacitors. The values of Q and Cdl recorded low digits with the iron alloy that has high nickel content, which further confirms that the increase of nickel content in the iron alloy increases its corrosion resistance.

Table 1. EIS parameters obtained for the Fe64/Ni36 and Fe55/Ni45 alloys.

Alloy	EIS Parameter					
	R_S / Ω	Q		R_{P1} / Ω	C_{dl} / μF	R_{P2} / Ω
		Y_{Q1}/ μF	n_1			
Fe64/Ni36	19.61	0.4153	0.80	72.75	8.296	700.10
Fe55/Ni45	21.3	0.1165	0.68	723	3.448	25570

Figure 4 shows (a) Bode impedance of the interface, |Z|, and (b) Bode degree of phase angle (Φ) plots obtained for (1) Fe64/Ni36 and (2) Fe55/Ni45 alloys immersed in 4% NaCl solutions for 40 min. It is well known that the high values of |Z|, particularly at the low frequency regions gives indications on a better corrosion resistance of a material. Also, the higher the values of Φ particularly at maximum, confirms the increased corrosion resistance. Since the curves of Figure 4 clears that the obtained values of |Z| as well as the values of Φ at almost all frequency regions for Fe55/Ni45 alloy (curves 2) are much higher than those for the Fe64/Ni36 alloy (curves 1), the corrosion resistance of Fe55/Ni45 alloy is very high compared to the corrosion resistance of Fe64/Ni36 alloy in the chloride test solution. The EIS Nyquist and Bode plots confirm that the iron alloy with higher nickel content provides more corrosion resistance compared to the low nickel content one in 4.0% sodium chloride solution.

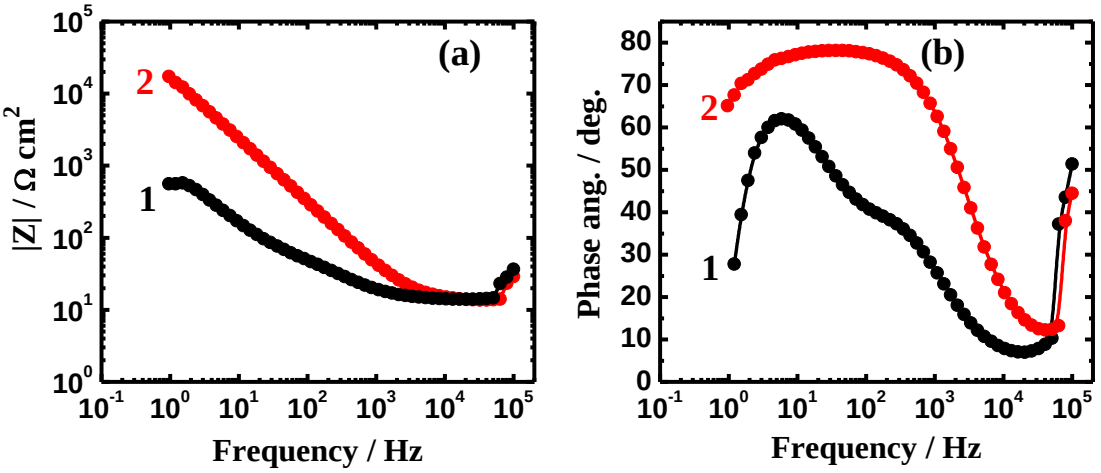

Figure 4. (a) Bode impedance of the interface, |Z|, and **(b)** Bode degree of phase angle plots for (1) Fe64/Ni36 and (2) Fe55/Ni45 alloys immersed in 4% NaCl solutions for 40 min.

3.3. Cyclic potentiodynamic polarization measurements

Cyclic potentiodynamic polarization (CPP) method has been successfully used to report the corrosion of metals and alloys in corrosive media [9,10]. The CPP curves obtained for iron nickel alloys, (1) Fe64/Ni36 and (2) Fe55/Ni45 immersed in 4% NaCl solutions for 40 min are shown in Figure 5. The corrosion parameters such as cathodic Tafel (β_c) slope, anodic Tafel (β_a) slope, corrosion potential (E_{Corr}), corrosion current density (j_{Corr}), polarization resistance (R_p), and corrosion rate (R_{Corr}) that were obtained from the CPP curves are depicted in Table 2. The values of E_{Corr} and j_{Corr} were obtained from the polarization curves as early reported [19,23]. The polarization resistance, Rp, values were calculated according the following relation [27]:

$$Rp = \frac{1}{j_{Corr}} \left(\frac{\beta_c \beta_a}{2.3 (\beta_c + \beta_a)} \right) \quad (1)$$

The values of the corrosion rate were calculated according to the following equation [26]:

$$R_{Corr} = j_{Corr} \left(\frac{k E_W}{d A} \right) \quad (2)$$

Where, k is a constant that defines the units for the corrosion rate (k = 128,800 milli inches (amp cm year)), E_W the equivalent weight in grams/equivalent of iron/nickel alloys (= 22.48 for Fe64/Ni36 and 23.44 for Fe55/Ni45), d the density in gcm^{-3} (8.19 for Fe64/Ni36 and 8.29 for Fe55/Ni45), and A the area of electrode is 1.0 in cm^2.

It is seen from Figure 5 that the obtained currents for the Fe64/Ni36 alloy are higher than those current values recorded for Fe55/Ni45 alloy overall the whole range of the polarization curves. The decrease of the cathodic current with the increase of the applied potential till reaching the values of the corrosion currents is due to the reduction of oxygen on the surface of the iron/nickel alloys as follows [27,28]:

$$O_2 + 2H_2O + 4e^- = 4OH^- \quad (3)$$

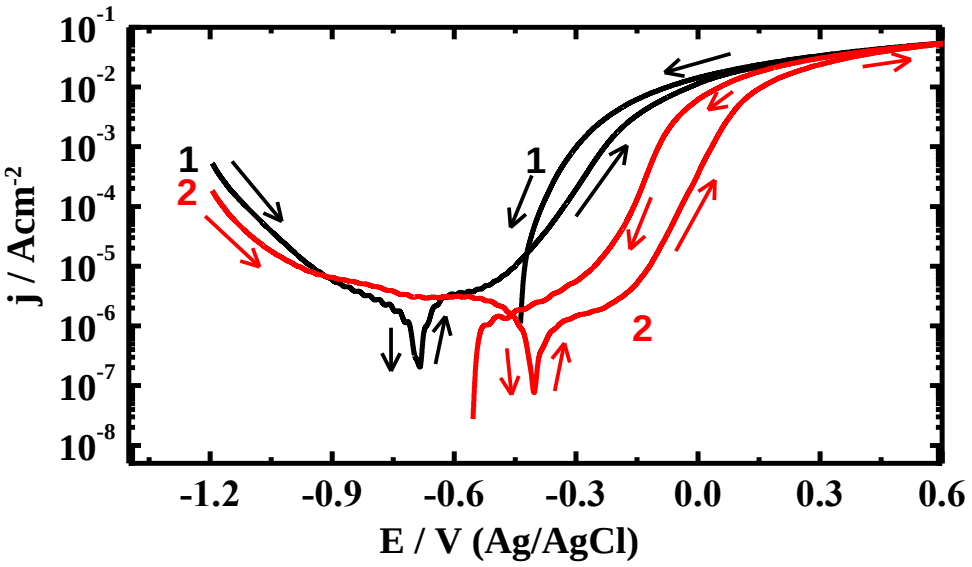

Figure 5. CPP curves recorded for iron-nickel alloy, (1) Fe64/Ni36 and (2) Fe55/Ni45 in 4% NaCl solutions.

Table 2. Corrosion data obtained from the polarization curves for Fe64/Ni36 and Fe55/Ni45 in 4.0% NaCl solutions.

Alloy	**Corrosion parameter**							
	β_c / V.dec^{-1}	E_{Corr} / V	β_a / V.dec^{-1}	j_{Corr} / µA cm^{-2}	E_{pit} / V	E_{prot} / V	R_p / kΩ	R_{Corr} / mpy
Fe64/Ni36	0.132	–0.700	0.110	0.90	-0.500	-0.260	28.99	0.318
Fe55/Ni45	0.148	–0.395	0.150	0.65	-0.420	-0.460	49.83	0.237

On the other hand, the increase of anodic currents with potential in the active region is due to the dissolution of metallic iron (Fe^0) from the alloy to ferrous cations (Fe^{2+}) as can be seen from these equations [28];

$$Fe = Fe^{2+} + 2e^- \quad (4)$$

Further increasing the potential towards the positive direction allows the alloy to form an oxide film as following,

$$Fe + ½\ O_2 + H_2O \rightarrow Fe(OH)_2 \quad (5)$$

$$3Fe(OH)_2 + ½\ O_2 \rightarrow Fe_3O_4 + 3H_2O \quad (6)$$

The formation of this oxide layer protects the surface of the alloy from harsh dissolution and explains the slow increase of currents with the increase of potential in the anodic direction. In compared to the previous studies by D. O. Condit [13] and Sayano and Nobe [14], the corrosion of iron-nickel alloys takes place by the same mechanism. Where, the dissolution of the alloy increases with the increase of iron content or the decrease of nickel in the alloy.

Reversing the applied potential led to increasing the obtained current in the backward direction indicating that these iron nickel alloys suffer severe pitting corrosion. The values of pitting potential (E_{Pit}) and protection potential (E_{Prot}) were also obtained from the polarization curves shown in Figure 5

and listed in Table 2. The corrosion data obtained from Figure 5 and recorded in Table 2 revealed that the values of j_{Corr} and R_{Corr} are higher for Fe64/Ni36 alloy compared to those obtained for Fe55/Ni45 alloy. Moreover, the value of corrosion resistance, Rp, of Fe64/Ni36 alloy is much lower than that calculated for Fe55/Ni45 alloy. Only the tendency for pitting corrosion for Fe55/Ni45 alloy was higher than that for Fe64/Ni36 alloy, which may be due to the alloy Fe55/Ni45 alloy is more passivated than Fe64/Ni36 alloy. This confirms the data obtained by EIS method that the increase of Ni content in iron alloy increases the resistance against corrosion in 4.0% NaCl solutions.

3.4. Chronoamperometric current-time at constant potential measurements

In order to report the effect of Ni content on the corrosion of iron/nickel alloys and whether pitting corrosion occurs in the sodium chloride solutions, 4.0%, the change of current with time experiments were carried out. The chronoamperometric curves obtained for (1) Fe64/Ni36 and (2) Fe55/Ni45 electrodes after their immersion in 4% NaCl solutions for 40 min minutes followed by applying a constant potential of 50 mV for 60 min are shown in Figure 6. It is seen that Fe64/Ni36 alloy (curve 1) recorded high current value (~17 mA/cm^2) upon the application of the constant potential value and slightly increased with time. This resulted from the dissolution of iron from the surface of the alloy as represented by Eq. (4). Further increase of the time led to a slight decrease of current values, which is due to the development of a corrosion product layer on the surface of the alloy.

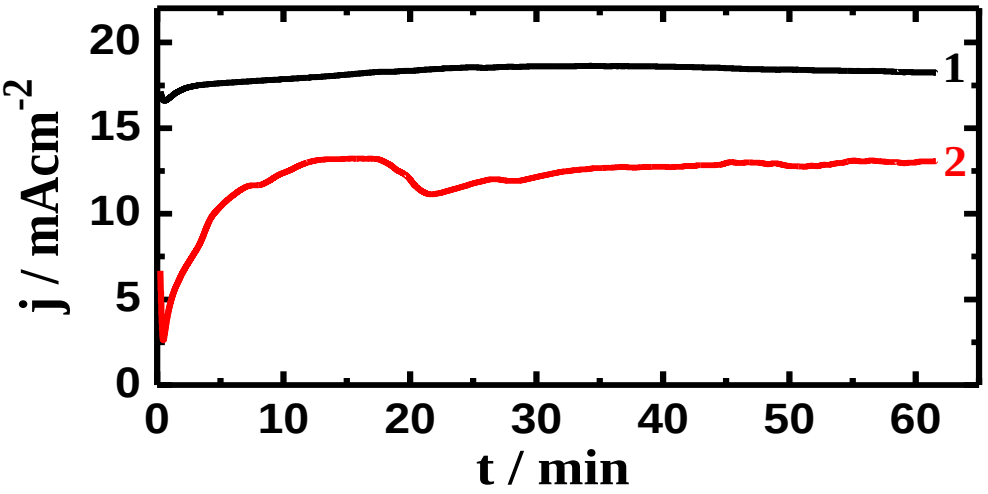

Figure 6. Current time curves for (1) Fe64/Ni36 and (2) Fe55/Ni45 alloys immersed in 4% NaCl solutions for 40 min minutes followed by applying a value of 50 mV for 60 min.

It is also seen from curve 2 (Figure 6) that the obtained current upon the application of potential on Fe55/Ni45 alloy was much lower (~8 mA/cm^2) than that obtained for Fe64/Ni36 alloy. This indicates that the surface of the Fe55/Ni45 alloy has more corrosion resistance against the corrosiveness attack of the chloride solution. Increasing the time of the applied potential led to

increasing the current values, which is most probably due to the dissolution of an air oxide film on the surface of the alloy. The current values then decreased before being stabilized till the end of the run. The decrease of current at this condition resulted from the formation of an oxide film and/or corrosion product layer that protects the surface from being attacked and corroded via chloride ions attack. The current-time behavior for both the iron/nickel alloys don't show any tendency towards the pitting corrosion as well as the absolute current values for Fe55/Ni45 alloy were much lower than the values obtained from Fe64/Ni36 alloy. The chronoamperometric current-time measurements thus confirm the data obtained from open-circuit potential, EIS, and polarization measurements. Where, the alloy that had high nickel content shows high corrosion resistance and that its uniform corrosion and pitting attack are low.

3.5. Scanning electron microscope (SEM) and energy dispersive X-ray analyzer (EDX)

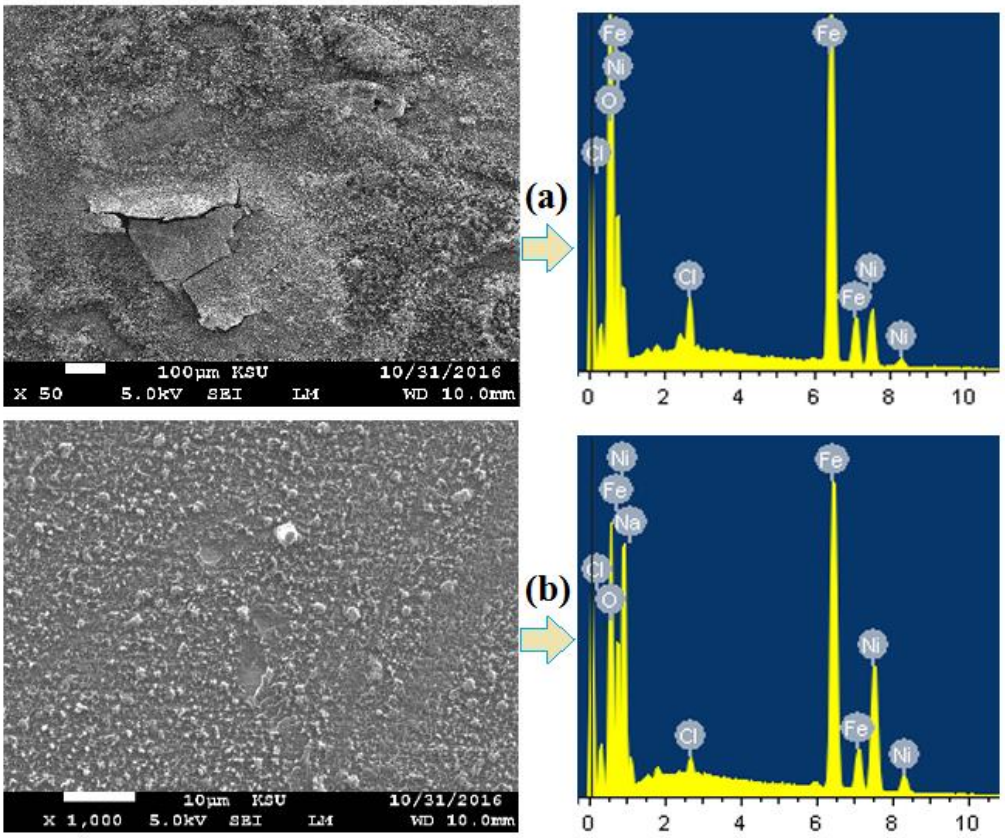

Figure 7. (a) SEM micrograph for the majority of the surface and the corresponding EDX spectra, while (b) represents the SEM image and EDX spectra for a small area of the surface has low corrosion product layers for Fe64/Ni36 alloy after its immersion in 4.0% NaCl solutions for 7 days.

The SEM and EDX investigations were carried out to report the surface morphology and the corrosion products found on the surface of iron/nickel alloys after long immersion period in the acid solution. Figure 7 shows (a) SEM micrograph for the majority of the surface and its corresponding

EDX profile analysis, while (b) represents the SEM image and EDX profile analysis for a small area of the surface has low corrosion product layers; (a) and (b) are for of the Fe64/Ni36 alloy after being immersed in 4.0% NaCl solutions for 4 days. Similar SEM images and EDX profiles were obtained for the surface of the Fe55/Ni45 alloy at the same conditions as shown in Figure 8.

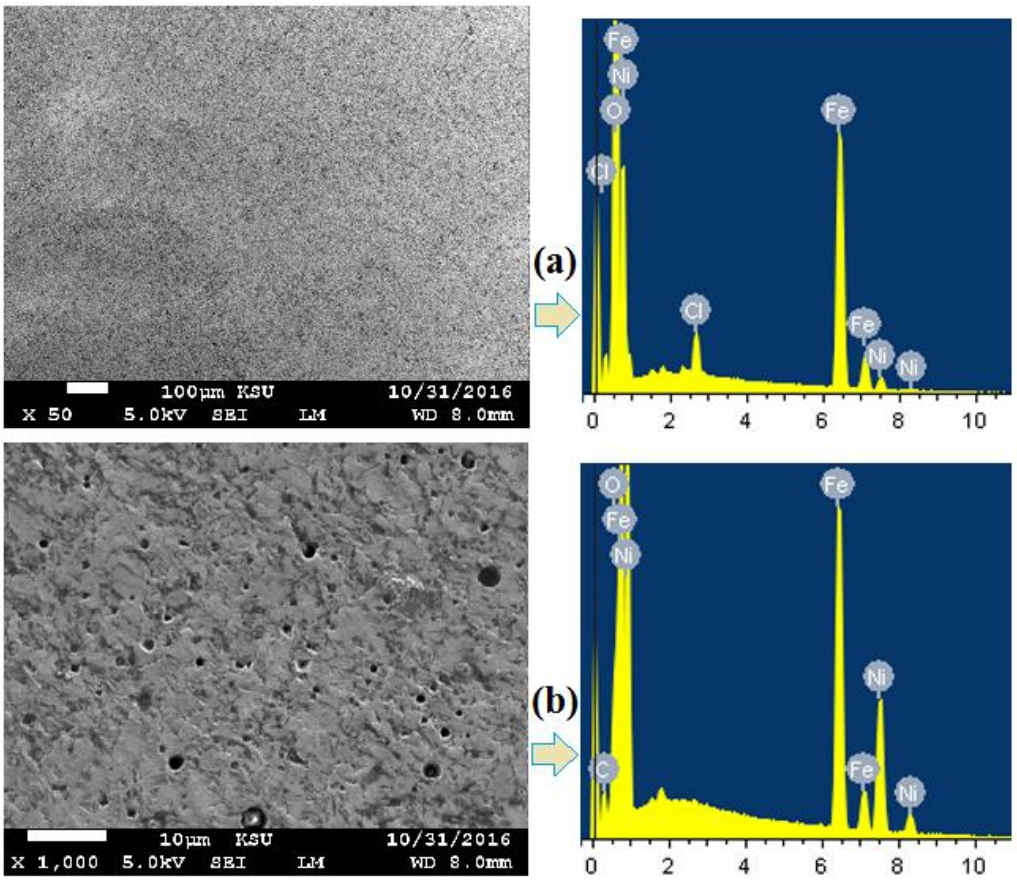

Figure 8. (a) SEM micrograph for the majority of the surface and its corresponding EDX spectra, while (b) represents the SEM image and EDX spectra for a small area of the surface has low corrosion product layers for the Fe55/Ni45 alloy after immersion in 4.0% NaCl solutions for 7 days.

It is seen from Figure 7 that the majority of the surface has thick corrosion product layers that cover all the surface of the Fe64/Ni36 alloy; analyzing these layers provided 45.39 wt.% Fe, 25.72 wt.% O, 11.77 wt.% Ni, and 17.12 wt.% Cl. This gives a suggestion that the corrosion products are mainly iron oxide and iron chloride. The low percentage of Ni indicates also that the majority of the surface is cover with a thick layer of corrosion products. The SEM and EDX data obtained for the small surface area shown in Figure 7 (b) indicated that only few places are not well covered with corrosion products. The weight percent (wt.%) for the elements found on the uncovered surface with corrosion products was 35.32 Fe, 45.53 Ni, 11.39 O, 5.66 Cl, and 2.11 Na. This tells us that the surface has low Fe and more Ni, which is most probably due to the dissolution of iron from the surface and the formation of iron oxide and iron chloride. Also, the presence of Na suggests that the surface still had some NaCl salt deposited on the surface.

The SEM/EDX results shown in Figure 8 (a) indicated that the morphology of a large area of the surface for Fe55/Ni45 alloy has large number of small pits as a result of the long immersion time of the alloy in the chloride solution. The pits have formed due to the aggressiveness attack of the chloride ions on the passivated areas of the surface of the alloy. The weight percents found on the surface of the alloy were 55.33 Fe, 4.29 Ni, 28.05 O, and 12.33 Cl. The high % of Fe as well as O confirms that the surface has iron oxide, which covers the whole surface and explains the low % of Ni. On the other hand, the morphology of an extended area of the surface of Fe55/Ni45 alloy (Figure 8b) shows a uniform distribution of corrosion products. The EDX profile analysis proved that the weight% for the elements found on the surface of the Fe55/Ni45 alloy were 49.88 Fe, 39.17 Ni, 6.06 C, and 4.89 O. The high content of Fe and Ni on the surface of the alloy proves that Fe55/Ni45 alloy is well protected against corrosion. The surface morphology as well as the EDX analysis for the Fe64/Ni36 and Fe55/Ni45 alloys in NaCl solutions suggest that the alloy does not show pitting corrosion and the uniform corrosion is very less due to the formation of corrosion products cover the surface and prevent it from being attacked by chloride ions.

4. CONCLUSIONS

In this study, the corrosion of Fe64/Ni36 and Fe55/Ni45 alloys in 4.0% NaCl solution using various electrochemical and spectroscopic techniques has been reported. OCP measurements showed a potential difference of about more than 100 mV vs. Ag/AgCl in the less negative direction for Fe55/Ni45 alloy compared to Fe64/Ni36 alloy. EIS method indicated that Fe55/Ni45 alloy has higher surface and polarization resistances than Fe64/Ni36. CPP experiments depicted that the corrosion current and corrosion rate recorded higher values for Fe64/Ni36 than those obtained for Fe55/Ni45 alloy. The absolute current values obtained for Fe55/Ni45 alloy at 50 mV vs. Ag/AgCl were much low as compared to the values obtained for Fe64/Ni36 under the same conditions. All results were good agreement with each other showing clearly that the alloy with high nickel content, which is Fe55/Ni45 alloy, has more resistance against corrosion than the alloy with lower nickel content in 4.0% NaCl solution.

ACKNOWLEDGEMENT
The authors would like to extend their sincere appreciation to the Deanship of Scientific Research at King Saud University for its funding of this research through the Research Group Project No. RGP-160.

References

1. D. Jiles, Introduction to magnetism and magnetic materials, *London, UK*: Chapman & Hall; 1994.
2. E. P. Wohlfarth, *J. Magnet. Magn. Mater.,* 10 (1979) 120-125.
3. O. Yamada, F. Ono, I. Nakai, Physica B+C, 91 (1977) 298-301.
4. O. Yamada, I. Nakai, F. Ono, *J. Magnet. Magn. Mater.,* 10 (1979) 155-156.
5. L. L. Hamer, *Adv. Mater. Process.,* 151 (1997) 31-34.
6. C. Woolger, *Mater. World*, 4 (1996) 332-333.

7. S.-H. Kim, H.-J. Sohn, Y.-C. Joo, Y.-W. Kim, T.-H. Yim, H.-Y. Lee, T. Kang, *Surf. Coat. Technol.*, 199 (2005) 43-38.
8. Lv Jinlong, Liang Tongxiang, Wang Chen, *Energy*, 112 (2016) 67-74.
9. B. Gehrmann, H. Hattendorf, A. Kolb-Telieps, *Mater. Corros.*, 48 (1997) 535–541.
10. Hiroyuki Konishi, Masato Yamashita, Hitoshi Uchida, Jun'ichiro Mizuk, *Mater. Trans.*, 46 (2005) 329–336.
11. Yoshinao Ihara, Hideji Ohgame, Kazutaka Sakiyama, Koji Hashimoto, *Corros. Sci.*, 22 (1982) 901–912.
12. M. Seo, H. Habazaki, T. Nakayama, *J. Solid State Electrochem.*, 20 (2016) 3133-3142.
13. D. O. Condit, *Corros. Sci.*, 12 (1972) 451-462.
14. R. R. Sayano, Ken Nobe, *Corrosion*, 25 (1969) 260-266.
15. El-Sayed M. Sherif, Abdulhakim A. Almajid, *J. Chem.*, 2014 (2014) 7.
16. El-Sayed M. Sherif, Jabair Ali Mohammed, Hany S. Abdo, Abdulhakim A. Almajid, *Int. J. Electrochem. Sci*., 11 (2016) 1355-1369.
17. El-Sayed M. Sherif, Hany S. Abdo, Jabair Ali Mohammed, Abdulhakim A. Almajid, Asiful H. Seikh, *Int. J. Electrochem. Sci*., 11 (2016) 4598-4610.
18. El-Sayed M. Sherif, Hany S. Abdo, Khalil A. Khalil, Ahmed M. Nabawy, *Int. J. Electrochem. Sci*., 11 (2016) 4632-4644.
19. El-Sayed M. Sherif, *Int. J. Electrochem. Sci*., 7 (2012) 4834-4846.
20. V. Shinde, P.P. Patil, *Mater. Sci. Eng. B*, 168 (2010) 142.
21. K.A. Khalil, El-Sayed M. Sherif, A.A. Almajid, *Int. J. Electrochem. Sci*., 6 (2011) 6184.
22. K. Darowicki, S. Krakowiak, P. Ślepski, *Electrochim. Acta*, 49 (2004) 2909.
23. El-Sayed M. Sherif, H.S. Abdo, K.A. Khalil, A.M. Nabawy, *Metals*, 5 (2015) 1799.
24. W. Gao, S. Cao, Y. Yang, H. Wang, J. Li, Y. Jiang, *Thin Solid Films*, 520 (2012) 6916.
25. El-Sayed M. Sherif, H.S. Abdo and A.A. Almajid, *Materials*, 8 (2015) 2127.
26. F.L. Floyd, S. Avudaiappan, J. Gibson, B. Mehta, P. Smith, T. Provder, J. Escarsega, *Prog. Org. Coat.*, 66 (2009) 8.
27. F.H. Latif, El-Sayed M. Sherif, A.A Almajid, H. Junaedi, *J. Anal. Appl. Pyrolysis*, 92 (2011) 485.
28. El-Sayed M. Sherif, R.M. Erasmus, J.D. Comins, *Electrochim. Acta*, 55 (2010) 3657–3663.